Journal of Cultural Heritage 64 (2023) 113–119

Contents lists available at ScienceDirect

Journal of Cultural Heritage

journal homepage: www.elsevier.com/locate/culher

Case study

Decay products of historical cements from the Palace of Knossos, Crete, Greece

Fernanda Carvalho[a,b,*], Maria Margarida R.A. Lima[a,b], Elissavet Kavoulaki[c], Nuno Leal[d], Joaquim Simão[d], Carlos Galhano[d], Hugo Águas[a,b], Giuseppina Padeletti[e], João Pedro Veiga[a,f,*]

[a] Materials Research Centre (CENIMAT/i3N), NOVA School of Science & Technology – FCT NOVA, 2829-516 Caparica, Portugal
[b] Department of Materials Science, NOVA School of Science & Technology – FCT NOVA, 2829-516 Caparica, Portugal
[c] EPHORATE of Antiquities of Heraklion, Xanthoudidou & 1 Chatzidaki str, Heraklion 71202, Greece
[d] GEOBIOTEC and Earth Sciences Department, NOVA School of Science & Technology – FCT NOVA, 2829-516 Caparica, Portugal
[e] National Research Council (CNR), Institute of Nanostructured Materials (ISMN), 10 Via Salaria km 29.5, 00015 Monterotondo, Roma, Italy
[f] Department of Conservation and Restoration, NOVA School of Science & Technology – FCT NOVA, 2829-516 Caparica, Portugal

ARTICLE INFO

Article history:
Received 13 February 2023
Accepted 18 September 2023
Available online 28 September 2023

Keywords:
Cement
Chemical characterization
Heritage building
Archaeological site

ABSTRACT

The Palace of Knossos, located on the island of Crete, Greece, is one of Europe's most important archaeological sites, serving as a testament to the Minoan civilization. Situated near the Mediterranean Sea, it is in close proximity to the seaport, airport, and industrial areas. Decay products commonly found in historical monuments within or near urban areas, such as black crusts and salt efflorescence, are also prevalent at the Palace of Knossos. To better understand the characteristics of the type of deterioration compounds found on cement in historical reconstruction zones, as well as their possible relationship with factors influencing the deterioration process, a multi-analytical approach was designed for the study of these materials. The results indicate that the black crusts primarily consist of gypsum and carbonaceous matter. However, the efflorescence salts are predominantly composed of thenardite instead of halite, despite the palace's proximity to the coastal area. These results may contribute to ongoing and future maintenance and preservation efforts for the monument.

Introduction

Decay crusts and salt efflorescence are commonly found in historical monuments located in or near urban areas [1]. Several factors influence the decay process of exposed materials, including pollutant type and concentration in the atmosphere, weather conditions, marine environment influence, bio receptivity, and the chemical-physical and mineralogical characteristics of the base material [1,2]. Pollutants such as NO_x, SO_2 and CO_2 react with air humidity, leading to the formation of secondary acidic components, particularly harmful to stone materials, mortars and cement [2,3].

Black crusts usually accumulate in sheltered areas of the monuments that are shielded from direct rain exposure and are more common in urban environments [4,5]. The most common type of black crusts results from the interaction between carbonated materials and SO_2 by-products, along with the carbonaceous fraction present in the air. This interaction leads to the formation of $CaSO_4{\cdot}2H_2O$ (gypsum) with embedded carbon particles, giving the layer its dark colour [1,3,6–10]. The irregularity and the porosity of the formed gypsum layer facilitate moisture penetration and the continuous deterioration process of the underlying material [3].

White crusts and efflorescence are also very common, with diverse compositions and complex mechanisms of interaction with the base materials, pollutants, or other sources of salts, such as marine spray or soil [5,11]. Generally, crusts exhibit more cohesiveness and stronger adhesion to the substrate, while efflorescence consists of less cohesive and more powdery crystals [5]. The crystallization of soluble salts is sensitive to temperature and humidity cycles of variation, leading to volume expansion within the pores of building materials and mechanical stress. This can result

* Corresponding authors.
E-mail addresses: fb.carvalho@campus.fct.unl.pt (F. Carvalho), jpv@fct.unl.pt (J.P. Veiga).

https://doi.org/10.1016/j.culher.2023.09.007

in damage such as cracking and detachment, especially in materials weakened by the passage of time [5,11–13].

Certain types of salts, such as thenardite, are commonly found in the deterioration process of construction materials, particularly calcium and sulphate-rich cement. Thenardite can pose a potential risk to porous materials, due to the process of dissolution and crystallization from the anhydrous phase to the hydrated phase, mirabilite. This process involves a complex equilibrium of phases, where the crystallization of the hydrated phase can generate pressure within the pores and cause damage to the materials [14–17]. Environmental conditions play a crucial role in maintaining this balance and influencing the crystallization of these two phases. The hydrated phase of this salt, mirabilite, exhibits greater stability under medium-high relative humidity conditions, particularly at lower temperatures. In contrast, thenardite is more stable under drier conditions and higher temperatures [15].

Considering the impact of environmental conditions, the identification of deteriorating compounds can be fundamental in defining monitoring and conservation strategies aimed at preventing or controlling this type of damage.

The Palace of Knossos: reconstruction materials

The Palace of Knossos in Crete is unique in its historical significance both as an archaeological site and for its restoration history. Excavations, conducted from the late 19th century to the early 20th century, revealed a vast built area with complex structures with diverse functions, rich in objects and remarkable finishing materials and decorations. The archaeological findings indicate that the Palace underwent distinct phases of construction and reconstruction between approximately 2000 and 1380 BCE, before being permanently destroyed by natural disasters [18]. Additionally, the remains discovered suggest that this same region continued to hold importance and was utilized during subsequent historical periods up to the Roman era [18,19].

Concurrent with the archaeological works starting from 1900, conservation interventions were carried out under the coordination of the archaeologist Sir Arthur Evans [20]. The conservation efforts were adapted over that period based on different architects' contributions and planning, availability of raw materials, and budget constraints. However, Evans' decision to reconstruct parts of the palace was motivated by two primary factors. Firstly it aimed to safeguard the structures that were being uncovered and exposed, fragile and sensitive to physical and environmental factors [21–24]. Secondly, the reconstruction was seen by Evans as an opportunity to showcase the true magnitude of the discovery and highlight the architectural and decorative achievements of the Minoan civilization [23,24].

The use of cement in the reconstruction, which proved to be more durable compared to initial attempts using wood in exposed areas, played a decisive role in Evans' decision to adopt reinforced concrete and expand the restoration efforts [23]. Cement was a modern, resilient material that could be moulded and was more cost-effective than importing wood for structural replacements.

However, despite being a more resilient material, the cement used in the Palace reconstruction, exposed to the weather conditions of the island, presented some issues over time, resulting in different consequences [25]. Crete has a typical Mediterranean climate, characterized by mild and rainy winters, as well as relatively warm and dry summers. From 1955 and 2010, average minimum temperatures ranged from 9 to 22 °C, while average maximum temperatures varied from 15 to 29 °C. In terms of average monthly precipitation, the highest values were recorded in January, reaching 90 mm, while average minimum values dropped below 1 mm in July. Relative humidity fluctuates between 55% in June and 70% in December [26]. Despite its proximity to the coastal area, the Palace

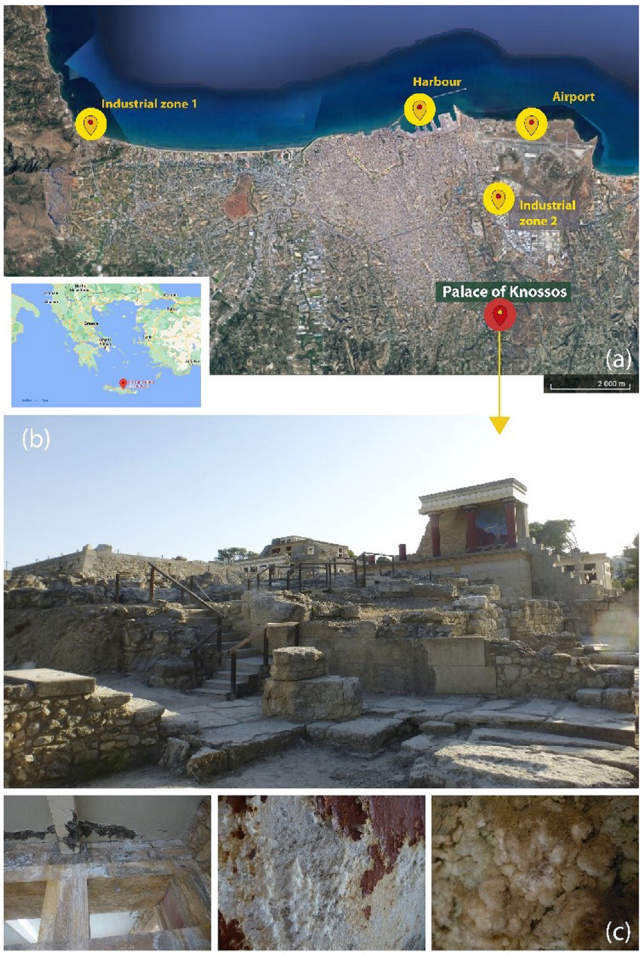

Fig. 1. (a) Location of the Palace of Knossos in relation to the pollution sources of Heraklion; (b) general view of one of the reconstructed parts of the Palace of Knossos; (c) decay products on cement and stones structures inner zones of reconstructions areas (Image/adapted from Google Earth and Google Maps, date image and maps ©2022 Google, HERACLES Project and F. Carvalho).

was built on top of the Kefala hill, providing geographical protection from direct Maritime influence [18]. Presently, it is located approximately 6 km from downtown Heraklion, in close proximity to the island's airport, harbour, and two industrial zones of the city (Fig.1).

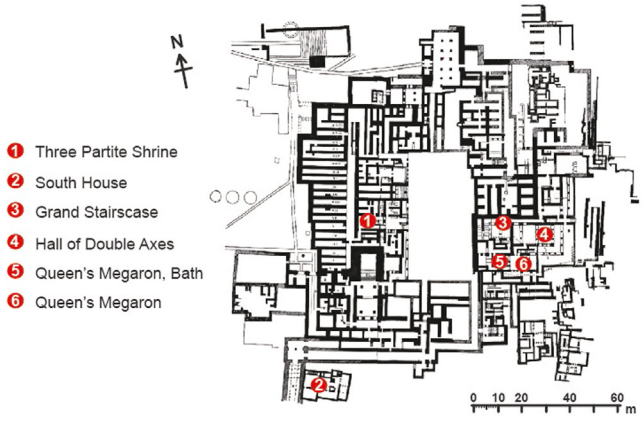

Fig. 2. Location of the sampling areas of the decay material of the concrete structures. (Image adapted from HERACLES Project and F. Carvalho et al. [27]).

Research aims

The primary objective of this study was to identify the types of decay products that occur as a result of deterioration processes on cement/concrete structures in the reconstructed areas of the Palace of Knossos. The secondary objective is to establish a correlation between these findings and the monument's location in order to comprehend the regional influence on the formation of specific types of crusts.

Methodology: materials and methods

The samples were collected from covered areas sheltered from direct rainfall. A total of seven samples of black crusts and eleven samples of white crusts and/or efflorescence accumulated were taken from the surfaces of pillars and other structures in six different areas of the Palace of Knossos (Fig.2), varying in terms of height and orientation (Table 1). The samples were categorized into three groups: black crust (BC), efflorescence (EF) and salt accumulation (SA). The black crust samples consist of cohesive fragments from the collected layer while the efflorescence samples are pulverulent and disaggregated. The samples identified as salt accumulation refer to white crusts, which are generally more cohesive and adherent to the substrate. To analyse these samples a multianalytical and multidisciplinary approach was designed. The smallest possible amount of sample was manually ground for analysis and techniques capable of preserving the samples were utilized during the process.

As received samples were observed under a stereo microscope to perceive their visual characteristics, using a Leica S9I Gree-

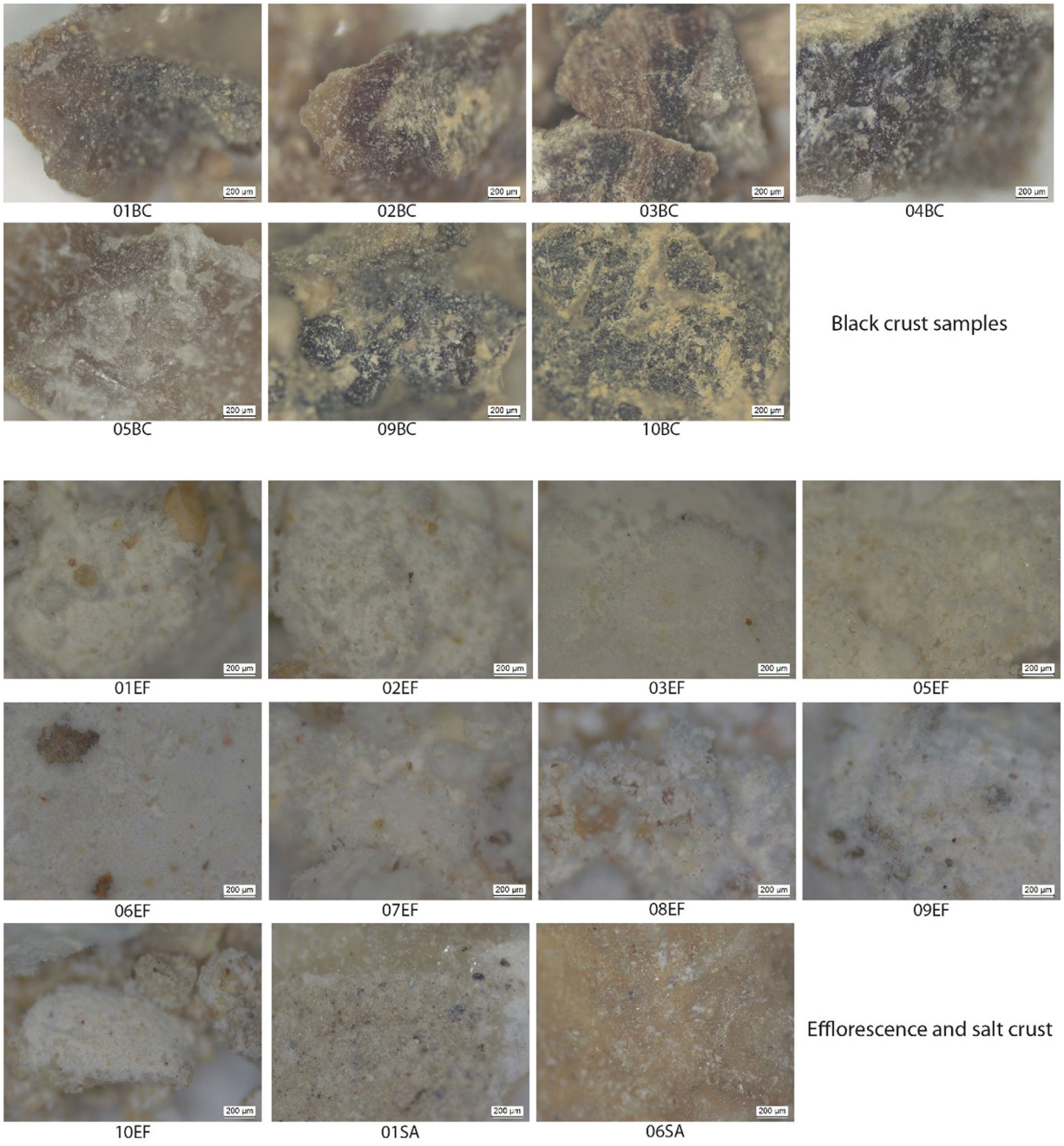

Fig. 3. Observation of samples in stereo microscope. It is possible to perceive the visual similarity between the samples according to the type of decay product.

nough Stereomicroscope, with Leica apochromatic lens, with a focal length of 50 mm, diameter of 58 mm and magnification of 5.50x.

For elemental chemical analysis, X-ray fluorescence was performed using a PANalytical – Axios 4.0X-ray fluorescence spectrometer with a wavelength dispersive system (WDXRF), with a rhodium X-ray tube (20.21 keV), in conditions optimized for element quantification. Fluorescent X-ray peaks were separated using LiF220, LiF200, Ge, PE, and PX1 analysing crystals to cover the entire measurable range. Analysis was performed under a He flow, and spectra deconvolution was performed using the iterative least-squares method. Standardless semiquantitative analysis based on the fundamental parameter approach was performed using the SuperQ software package (PANalytical B.V., Almelo, The Netherlands).

X-ray diffraction (XRD) analysis for the identification of mineralogical phases in the samples was performed using a Rigaku diffractometer, model DMAX III-C 3 kW, with Cu Kα radiation at 40 kV and 30 mA settings, in the 2θ range of 10° to 65°, with a step of 0.08° and an acquisition time of 1 s per step, in continuous scan mode. The identification of results was carried out using the X'Pert High Score Plus software.

Fourier-transform infrared spectroscopy (FTIR) was used as an auxiliary technique for identifying the characteristic molecular vibrations bands of sample components. Data was recorded using an attenuated total reflectance (ATR) sampling accessory (Smart iTR) equipped with a single bounce diamond crystal on a Thermo Nicolet 6700 Spectrometer. Spectra were acquired in the range of 4000–525 cm^{-1} with a 4 cm^{-1} resolution.

Raman spectroscopy measurements were conducted to identify the main components of the samples. The analyses were performed using a Renishaw inVia Qontor micro-Raman spectrometer, equipped with an air-cooled CCD detector and a HeNe laser operating at 32 mW for 633 nm laser excitation. The spectral resolution of the spectroscopic system is 0.3 cm^{-1}. The laser beam was focused with 50x or 100x Olympus objective lens (N10.6 LMPLAN FL N). The raw data were digitally collected using Wire 5.1 software for processing. The interpretation of the results was carried out by comparing the obtained spectra with the RRuff database and relevant literature.

Discussion of results

The visual observation under stereo microscope revealed similarities and differences amongst the groups of samples, according to sampling classification. In the case of black crusts, there was a visual variation in colour intensity, ranging from darker tones, as observed in samples 04BC, 09BC and 10BC, to lighter brown, as observed in sample 05BC (Fig. 3). The samples exhibited heterogeneity.

The observed efflorescence samples displayed a non-cohesive layer composed of fine, white, and opaque crystals, accumulated heterogeneously on the surface of the substrate (Fig. 3). In contrast, the two samples of white crusts, 01SA and 06SA, differed visually from the efflorescence samples. The deteriorated layer in these samples appeared more cohesive, particularly in sample 06SA (Fig. 3). Sample 06SA also exhibited a more yellowish colour, and crystals observed on its surface were distinct, with elongated and translucent crystals predominating, compared to the 01SA sample.

WDXRF analysis provided the average elemental chemical composition of historical Portland cement samples used in the reconstructions, revealing that they primarily consisted of CaO accounting for more than 75% of their composition (Fig. 4a). Examining the decay products, as expressed in oxides, it was found that black crusts have the highest percentages of SO_3, ranging from 46% to 57%. Similarly, samples of white crusts showed percentages of SO_3 at 51% and 55% for the two samples of this typology (01SA and 06SA). Efflorescence samples show the presence of Na_2O with levels ranging from 16% to 27% (Fig. 4b). Furthermore, the efflorescence samples displayed the greatest variation in CaO percentages, ranging from 36% to 68%. In contrast, black and white crust samples exhibited CaO percentages between 41% and 47%. The efflorescence samples also showed higher percentages and greater variations in the values of Fe_2O_3, Al_2O_3 and SiO_2 when compared to the crust samples (Fig. 4b).

The XRD results (Table 1), indicate that the main crystalline phase identified in the samples of black crusts was gypsum ($Ca(SO_4)\cdot 2H_2O$), with the highest intensity peaks observed in all samples. Additionally, anhydrite ($Ca(SO_4)$), calcite ($CaCO_3$) and quartz (SiO_2) were also identified as crystalline phases in almost all samples of black crusts, although with lower intensity peaks. The presence of anhydrite in cement deterioration materials has been previously reported by other authors and may be attributed to various factors, including the impact of temperatures above 40ºC during summer, which can trigger gypsum dehydration processes [28]. Two samples also exhibited very low intensity peaks of thenardite (Na_2SO_4). These findings are consistent with the semi-quantification obtained by WDXRF and the visual similarities observed in this type of sample. In the case of

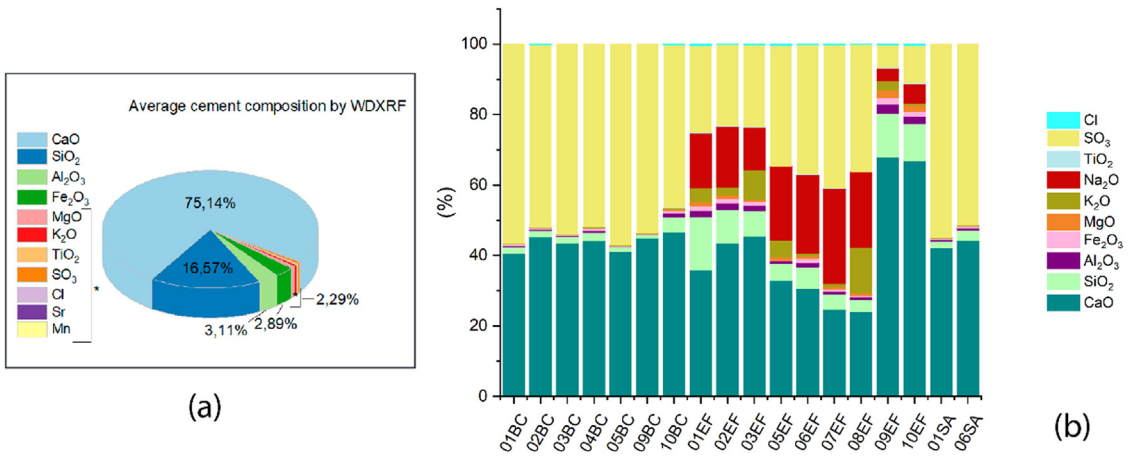

Fig. 4. (a) Average cement composition determined by WDXRF. (b) Elemental distribution determined by WDXRF for samples under study. The samples of black and white crusts present the highest percentages of sulphur, while the efflorescence samples have the highest percentages in sodium and chlorine.

Table 1
Crystalline phases identified by XRD, according to peak intensity, for samples of black crusts, efflorescence, and saline white crusts. Calcite (Cal), Dolomite (Dol), Feldspar (Fsp), Quartz (Qz), Hematite (Hem), Gypsum (Gp), Anhydrite (Anh), Thenardite (Thn), Syngenite (Sgn) and Aphthitalite (Att) [31].

Sample	Location*	Cal	Dol	Fsp	Qz	Hem	Gp	Anh	Thn	Sgn	Att
Cement	–	+++++		+	+++	+					
01BC	1.5 m, N	+			+		+++++	++			
02BC	0.8 m, S						+++++	+++			
03BC	0.2 m, W	+					+++++		+		
04BC	1.5 m, E	+			+		+++++		+		
05BC	1.5 m, N						+++++	+			
09BC	1.5 m, E	+					+++++	++			
10BC	1.5 m, S	+			+		+++++	+			
01EF	2.5 m, W	++++			+++				+++	+	
02EF	2.0 m, E	+++++			+++				+++		
03EF	2.0 m, E	+++++		+++	++				+++	+	+
05EF	2.0 m, N	+++++	++	++					++++		+
06EF	3.0 m, S	++++			++				+++++	+	
07EF	2.5 m, N	+++++	++		++				+++		+
08EF	3.0 m, N	+++++	++	++	++				++++		+
09EF	3.0 m, E	+++++	+		++				++		
10EF	3.0 m, E	+++++		+	++				+		
01SA	2.0 m, N						+++++		+		
06SA	1.5 m, N	++	+				+++++		+		

* Approximate height and orientation of the built structure where the samples were taken.North (N), south (S), east (E), west (W)Intensity of diagnosis lines: Very intense (+++++); intense (++++); median intensity (+++); low intensity (++); very low intensity (+).

efflorescence samples, the main crystalline phase identified was thenardite. Other salts like syngenite ($K_2Ca(SO_4)\cdot 2H_2O$) and aphthitalite ($NaK_3(SO_4)_2$) were also detected in the efflorescence samples with higher potassium contents. These products are commonly associated with the deterioration of construction materials [29,30] and may occur in conjunction with thenardite.

The FTIR-ATR results (Fig. 5a) further support the presence of calcium sulphate dihydrate ($Ca(SO_4)\cdot 2H_2O$) as the main component in both black and white crusts. The spectra present characteristic stretching vibration bands of the OH^- group at approximately 3504 and 3398 cm^{-1}, as well as bending vibration bands of the same group at 1684 and 1618 cm^{-1}. Additionally, stretching vibration bands of the SO_4^{2-} are observed in the region of 1103 cm^{-1}, with the less intense band at 667 cm^{-1} [32–35]. As identified by XRD, the FTIR-ATR analysis of efflorescence samples confirms the presence of thenardite and calcite as the main components of these salts, with the thenardite bands having higher intensity compared to calcite bands. The characteristic stretching vibration bands of the SO_4^{2-} group for thenardite are observed in the region of 1097 and 1091 cm^{-1}, along with the bands at 609 and 636 cm^{-1} [36]. In the case of sample 05EF, the result also presents characteristic bands of the CO_3^{2-} group at 1425 cm^{-1} and 875 cm^{-1}, but they also present bands in the OH^- group vibration zone at 3454 cm^{-1} and 1678 cm^{-1} approximately, indicating the presence of additional components that have not been identified.

Raman spectroscopy results (Fig. 5b) confirm the presence of gypsum as the main mineral identified in the samples of black and white crusts. The characteristic vibration bands of the SO_4^{2-} group are observed at 1138, 1009, 622, 495 and 415 cm^{-1} [37,38]. It was also possible to identify in some samples, the vibration bands characteristic of carbon particles, wider and centred at 1360 and 1599 cm^{-1}, contributing to the colouration of the crust [37]. For the efflorescence samples, thenardite was identified in all samples, with the low-intensity vibration bands centred on 1155, 1133, 1105 cm^{-1}, the most intense band centred at 995 cm^{-1} and further low-intensity bands centred at 649, 635, 624, 468 and 454 cm^{-1} [36,37].

Concrete structures in Knossos are composed of cement, characterized by a low sulphur content and a high calcium percentage. The main mineral identified is Calcite. According to some authors, the deterioration of carbonate materials, leading to the formation of white and black gypsum crusts, is triggered by processes involving rainwater, CO_2, acid rain resulting from pollutants such as SO_2 and NO_x, and the dry deposition of gaseous pollutants [8,39–41]. Although cement is more resistant to acid attacks compared to limestone itself, it remains a porous material and susceptible to this type of reaction [40,42]. The material's porosity further contributes to increased interaction with water, as well as the penetration and circulation of alkaline ions and other salts originating from the concrete composition, or pollutants deposition. This phenomenon may explain the thenardite efflorescence salts. The dissolution, hydration and crystallisation processes of thenardite are sensitive to variations in relative humidity and temperature, with a greater dependency on higher temperatures and lower relative humidities [11]. According to the data published by the HERACLES project, Knossos experiences the largest daily temperature ranges on average during the spring months [43]. The proximity of Knossos to modern sources of pollution, such as the airport, harbour, and industrial areas of Heraklion, which did not exist in the early 20th century, has a direct impact on the type of decay material found at the archaeological site. The burning of fossil fuels associated with these activities contributes to the circulation of pollutants in the region [44]. Additionally, the proximity to the sea also plays a role in the transport of harmful particles. A study by Sakka et al. [45] focusing on the variability of aerosol spray in different archaeological sites in Greece, presents that in Knossos polluted dust, dust and clean marine spray are the predominant aerosols during spring. The statistical data on precipitation in the city of Heraklion, as published by the HERACLES project [36], show that on average the largest daily variations in wind speed are recorded in the late winter and early spring months. This factors together with speed and direction of wind, can play a key role in the transportation and deposition of salts over long distances. For example, the deposition of NaCl is significantly reduced in buildings located more than 200 m from the shoreline. Additionally, halite, originating from sea spray can rapidly react with atmospheric sulphur, resulting in the formation of thenardite. The predominance of thenardite identified in this study may be related both to the 6 km distance between the archaeological site and the coastline and to a higher availability of pollutants such as SO_2 in the atmosphere [46,47]. However, the distance from the coastline does not prevent the transportation of other types of pollutants.

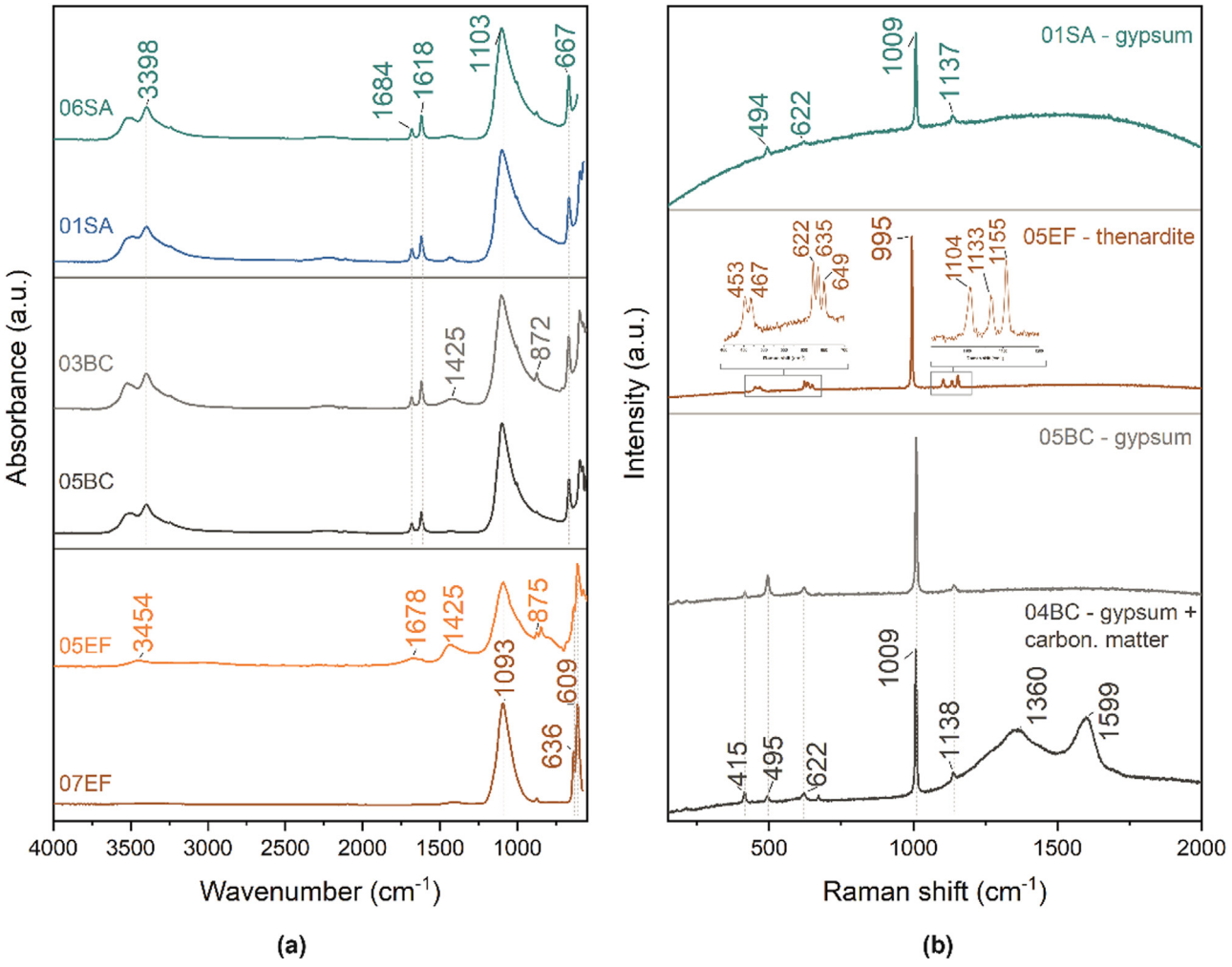

Fig. 5. (a) Main FTIR-ATR results obtained for each sample typology, being gypsum vibrations identified in the black and white crust samples and thenardite vibrations identified in the efflorescence samples. (b) main results obtained by μ-Raman, with the same components identified, in addition to carbonaceous matter together with gypsum.

Sakka et al. [45] also emphasize the impact of dust originating from North Africa as a pattern, with the island of Crete being one of the first sites affected by this type of pollutant.

Conclusion

The selection of materials for the reconstruction of the Palace of Knossos was based on various factors, including their characteristics, availability, technological advancements, and the knowledge available at the beginning of the 20th century. The choice of using cement and concrete was deliberate, considering their durability and resistance to external conditions. However, these materials are still susceptible to deterioration caused by weathering.

The characterisation of the samples collected at Knossos Palace indicates that the black and white crusts predominantly consist of gypsum. In the case of black crusts, there is also the presence of carbonaceous matter incorporated into the layer. The study also reveals that efflorescence is primarily composed of thenardite. The accumulation and crystallization of these salts result from the interaction between the underlying base material, atmospheric pollutants, marine aerosols, seasonal weather conditions, amongst other factors.

Identifying the specific types of deterioration present at the site helps in developing monitoring strategies and planning periodic maintenance activities. By understanding the types of salts involved and the seasonality of environmental conditions, appropriate measures can be implemented to mitigate further damage and preserve the historical site.

Funding

This work was supported by the FEDER funds through the COMPETE 2020 Programme and National Funds through FCT-Portuguese Foundation for Science and Technology under the project ref. UIDB/50025/2020-2023 and, SFRH/BD/145308/2019 (F. Carvalho), European Union Horizon 2020 research and innovation programme H2020-DRS-2015 GA nr.700395 (HERACLES project) and H2020 EIT Raw Materials MineHeritage Project (PA 18111).

References

[1] C.M. Belfiore, D. Barca, A. Bonazza, V. Comite, M.F. la Russa, A. Pezzino, S.A. Ruffolo, C. Sabbioni, Application of spectrometric analysis to the identification of pollution sources causing cultural heritage damage, Environ. Sci. Pollut. Res. 20 (2013) 8848–8859, doi:10.1007/s11356-013-1810-y.

[2] T. Yates, Mechanisms of air pollution damage to brick, concrete and mortar, in: P. Brimblecombe (Ed.), Eff. Air Pollut. Built Environ., Imperial College Press, London, 2003, pp. 107–132.

[3] F. Corvo, J. Reyes, C. Valdes, F. Villaseñor, O. Cuesta, D. Aguilar, P. Quintana, Influence of air pollution and humidity on limestone materials degradation in historical buildings located in cities under tropical coastal climates, Water. Air. Soil Pollut. 205 (2010) 359–375, doi:10.1007/s11270-009-0081-1.

[4] E.M. Perez-Monserrat, R. Fort, M.J. Varas-Muriel, Monitoring façade soiling as a maintenance strategy for the sensitive built heritage, Int. J. Archit. Herit. 12 (2018) 816–827, doi:10.1080/15583058.2017.1419312.
[5] V. Verges-Belmin, ICOMOS-ISCS: Illustrated Glossary on Stone Deterioration Patterns, ICOMOS International Scientific Committee for Stone (ISCS), Paris, 2008.
[6] J.S. Pozo-Antonio, C. Cardell, V. Comite, P. Fermo, Characterization of black crusts developed on historic stones with diverse mineralogy under different air quality environments, Environ. Sci. Pollut. Res. 29 (2022) 29438–29454, doi:10.1007/s11356-021-15514-w.
[7] V. Comite, A. Miani, M. Ricca, M.La Russa, M. Pulimeno, P. Fermo, The impact of atmospheric pollution on outdoor cultural heritage: an analytic methodology for the characterization of the carbonaceous fraction in black crusts present on stone surfaces, Environ. Res. 201 (2021) 111565, doi:10.1016/j.envres.2021.111565.
[8] A.E. Charola, J. Pühringer, M. Steiger, Gypsum: a review of its role in the deterioration of building materials, Environ. Geol. 52 (2007) 339–352, doi:10.1007/s00254-006-0566-9.
[9] J. Sanjurjo-Sánchez, C. Alves, Decay effects of pollutants on stony materials in the built environment, Environ. Chem. Lett. 10 (2012) 131–143, doi:10.1007/s10311-011-0346-y.
[10] M. Bouichou, E. Marie-Victoire, Cleaning Historic Concrete: A Guide to Techniques and Decision-Making, J. Paul Getty Trust, Los Angeles, 2021.
[11] A.E. Charola, Salts in the deterioration of porous materials: an overview, J. Am. Inst. Conserv. 39 (2000) 327–345, doi:10.1179/019713600806113176.
[12] E. Doehne, Salt weathering : a selective review, Geol. Soc. London, Spec. Publ. 205 (2002) 51–64, doi:10.1144/GSL.SP.2002.205.01.05.
[13] E. Ruiz-Agudo, F. Mees, P. Jacobs, C. Rodriguez-Navarro, The role of saline solution properties on porous limestone salt weathering by magnesium and sodium sulfates, Environ. Geol. 52 (2007) 269–281, doi:10.1007/s00254-006-0476-x.
[14] B. Lubelli, V. Cnudde, T. Diaz-Goncalves, E. Franzoni, R.P.J. van Hees, I. Ioannou, B. Menendez, C. Nunes, H. Siedel, M. Stefanidou, V. Verges-Belmin, H. Viles, Towards a more effective and reliable salt crystallization test for porous building materials: state of the art, Mater. Struct. Constr. 51 (55) (2018) 1–21, doi:10.1617/s11527-018-1180-5.
[15] L. Germinario, C.T. Oguchi, Gypsum, mirabilite, and thenardite efflorescences of tuff stone in the underground environment, Environ. Earth Sci. 81 (242) (2022) 1–12, doi:10.1007/s12665-022-10344-6.
[16] N. Tsui, R.J. Flatt, G.W. Scherer, Crystallization damage by sodium sulfate, J. Cult. Herit. 4 (2003) 109–115, doi:10.1016/S1296-2074(03)00022-0.
[17] N. Thaulow, S. Sahu, Mechanism of concrete deterioration due to salt crystallization, Mater. Charact. 53 (2004) 123–127, doi:10.1016/j.matchar.2004.08.013.
[18] Knossos2000-2008. Conservation, Consolidation and Promotion of the Palace and Archaeological Site, Knossos Scientific Committee, Heraklion, 2008.
[19] S. Hood, D. Smyth, Archaeological survey of the Knossos Area, Br. Sch. Athens. Suppl. 14 (1981) 1–69, doi:10.1556/ArchErt.132.2007.1.10.
[20] M. Panagiotaki, Knossos and Evans: buying Kephala, in: G. Cadogan, E. Hatzaki, A. Vasilakis (Eds.), 23rd Ephoreia Prehist. Class. Antiq. Herakleion, British School at Athens, Herakleion, 2000.
[21] A. Evans, The Palace of Minos at Knossos, Vol I, Macmillan and Co., London, 1921.
[22] A. Evans, The Palace of Minos at Knossos, Vol.IV, Oxford University Press, London, 1935 Part I.
[23] P. Kienzle, Conservation and Reconstruction at the Palace of Minos at Knossos, University of York, 1998.
[24] A. Karetsou, Knossos after Evans: past interventions, present state and future solutions, Br. Sch. Athens Stud. 12 (2004) 547–555.
[25] L. Bertolini, M. Carsana, M. Gastaldi, F. Lollini, E. Redaelli, Corrosion assessment and restoration strategies of reinforced concrete buildings of the cultural heritage, Mater. Corros. 62 (2011) 146–154, doi:10.1002/maco.201005773.
[26] Hellenic National Meteorological Service, (n.d.). http://emy.gr/emy/en/climatology/climatology_city?perifereia=Crete&poli=Heraklion (accessed January 16, 2023).
[27] F. Carvalho, P. Sousa, N. Leal, J. Simão, E. Kavoulaki, M.M. Lima, T.P. Silva, H. Águas, G. Padeletti, J.P. Veiga, Mortars from the Palace of Knossos in Crete, Greece: a multi-analytical approach, Minerals 12 (2022) 1–16, doi:10.3390/min12010030.
[28] M. Secco, G.I. Lampronti, M.C. Schlegel, L. Maritan, F. Zorzi, Degradation processes of reinforced concretes by combined sulfate-phosphate attack, Cem. Concr. Res. 68 (2015) 49–63, doi:10.1016/j.cemconres.2014.10.023.
[29] V. Matović, S. Erić, A. Kremenović, P. Colomban, D. Srećković-atoćanin, N. Matović, The origin of syngenite in black crusts on the limestone monument King's Gate (Belgrade Fortress, Serbia) - the role of agriculture fertiliser, J. Cult. Herit. 13 (2012) 175–186, doi:10.1016/j.culher.2011.09.003.
[30] H. Brocken, T.G. Nijland, White efflorescence on brick masonry and concrete masonry blocks, with special emphasis on sulfate efflorescence on concrete blocks, Constr. Build. Mater. 18 (2004) 315–323, doi:10.1016/j.conbuildmat.2004.02.004.
[31] L.N. Warr, IMA–CNMNC approved mineral symbols, Mineral. Mag. 85 (2021) 291–320, doi:10.1180/mgm.2021.43.
[32] F.B.B. de Carvalho, Levantamento e Caracterização de Adesivos e Materiais De Preenchimento Utilizados Na Preservação de Cerâmica Arqueológica Levantamento e Caracterização De Adesivos e Materiais De Preenchimento Utilizados Na Preservação de Cerâmica Arqueológica, Universidade Nova de Lisboa, 2016.
[33] J. Coates, Interpretation of infrared spectra, a practical approach, Encycl. Anal. Chem. (2000) 10815–10837, doi:10.1002/9780470027318.
[34] B.H. Stuart, Infrared Spectroscopy: Fundamentals and Applications, John Wiley & Sons, Chichester, 2004, doi:10.1002/0470011149.
[35] M.R. Derrick, D. Stulik, J.M. Landry, Infrared Spectroscopy in Conservation Science, J. Paul Getty Trust (1999).
[36] RRUFF, Thenardite R040178, (n.d.). https://rruff.info/thenardite/display=default/R040178 (accessed June 13, 2022).
[37] M. Marszałek, Identification of secondary salts and their sources in deteriorated stone monuments using micro-Raman spectroscopy, SEM-EDS and XRD, J. Raman Spectrosc. 47 (2016) 1473–1485, doi:10.1002/jrs.5037.
[38] S. Kramar, M. Urosevic, H. Pristacz, B. Mirtič, Assessment of limestone deterioration due to salt formation by micro-Raman spectroscopy: application to architectural heritage, J. Raman Spectrosc. 41 (2010) 1441–1448, doi:10.1002/jrs.2700.
[39] A. Bonazza, P. Messina, C. Sabbioni, C.M. Grossi, P. Brimblecombe, Mapping the impact of climate change on surface recession of carbonate buildings in Europe, Sci. Total Environ. 407 (2009) 2039–2050, doi:10.1016/j.scitotenv.2008.10.067.
[40] A. Bonazza, C. Sabbioni, A. Bonazza, C. Sabbioni, N. Ghedini, G. Gobbi, Blackening as major atmospheric pollution effect on monuments, Pollut. Atmosphérique (2007) 7–12.
[41] J. Chwast, J. Todorovic, H. Janssen, J. Elsen, J. Todorović, H. Janssen, J. Elsen, Gypsum efflorescence on clay brick masonry: field survey and literature study, Constr. Build. Mater. 85 (2015) 57–64, doi:10.1016/j.conbuildmat.2015.02.094.
[42] J. Broomfield, The identification and assessment of defects, damage and decay, in: S. Macdonald (Ed.), Concr. Build. Pathol., Blackwell Science, Oxford, 2003, pp. 140–160.
[43] H. Project, TEST-BED 1: Palace of Knossos, Heraklion, EL, 2018 http://www.heracles-project.eu/project-test-beds/test-bed-1-palace-knossos-heraklion-el (accessed May 26, 2023).
[44] Alexander Starik, Gaseous and particulate emissions with jet engine exhaust and atmospheric pollution, Adv. Propuls. Technol. High-Speed Aircr. 150 (2008) 1–22.
[45] A. Sakka, E. Gerasopoulos, E. Liakakou, I. Keramitsoglou, N. Zacharias, Spatial variability of aerosols over Greek archaeological sites using Space-Borne Remote Sensing, J. Cult. Herit. 46 (2020) 207–217, doi:10.1016/j.culher.2020.07.001.
[46] G.R. Meira, M.C. Andrade, I.J. Padaratz, M.C. Alonso, J.C. Borba, Measurements and modelling of marine salt transportation and deposition in a tropical region in Brazil, Atmos. Environ. 40 (2006) 5596–5607, doi:10.1016/j.atmosenv.2006.04.053.
[47] K.M. Anwar Hossain, S.M. Easa, M. Lachemi, Evaluation of the effect of marine salts on urban built infrastructure, Build. Environ. 44 (2009) 713–722, doi:10.1016/j.buildenv.2008.06.004.